Proceedings of the 28th IEEE
EMBS Annual International Conference
New York City, USA, Aug 30-Sept 3, 2006

Morphological Exponential Entropy Driven-HUM

Edoardo Ardizzone, Roberto Pirrone and Orazio Gambino

***Abstract*— This paper presents an improvement to the Exponential Entropy Driven - Homomorphic Unsharp Masking (E^2D-HUM) algorithm devoted to illumination artifact suppression on Magnetic Resonance Images. E^2D-HUM requires a segmentation step to remove dark regions in the foreground whose intensity is comparable with background, because strong edges produce streak artifacts on the tissues. This new version of the algorithm keeps the same good properties of E^2D-HUM without a segmentation phase, whose parameters should be chosen in relation to the image.**

I. INTRODUCTION

Most of the studies on illumination correction found in literature are oriented to brain [18] magnetic resonance images (mri). The knee mri are strongly affected by this artifact due to the particular coil configuration of specialized devices for upper and lower limbs. Two main approaches are used to suppress illumination inhomogeneity. The first kind of algorithms like[7][13][5] modify the expectation maximization or fuzzy c-means [10][4][16]. The original minimizing functional is changed to take into account the artifact corrupting the images, new parameters are introduced decreasing the original performance. The algorithms like [11][8][12][9] suppress the artifact making use of a particular probe inserted into the device to produce a correcting bias surface, other methods discover the artifact using methods based on information theory [14][15], preconditioned gradient algorithm [3], polynomial fitting [2] or an "a priori" model [17]. The paper is organized as follows: Section 2 describes briefly E^2D-HUM; Section 3 describes ME^2D-HUM; Section 4 perform a comparison among ME^2D-HUM, E^2D-HUM, SPM2 [20]; Section 5 is devoted to measures; Section 6 describes briefly the dataset; Section 7 reports some conclusions.

II. EXPONENTIAL ENTROPY DRIVEN - HOMOMORPHIC UNSHARP MASKING

A. Guillemaud Filter

The E^2D-HUM algorithm is described in [1]. In this section a brief explanation of the algorithm is given. E^2D-HUM is based on the Guillemaud filter (*Gf*) [6] consisting in a modified homomorphic filtering oriented to images composed by a dark background and a bright foreground, like most of medical images. This filter attenuates the bias avoiding the appearance of a streak artifact between foreground and background due to the edge. A scheme of such filter is given in fig.1. The log-filtered image is corrected by a filtered mask where the pixels whose pixels are 1 in correspondence of the Region Of Interest (ROI), that is the image foreground. A low pass configuration of the homomorphic scheme is preferred to a high pass one in such a way that an image of the bias is also obtained. The dynamics of the images resulting from the previous pipeline must be stretched to the original one. This obvious phase is omitted in the scheme.

Edoardo Ardizzone, Roberto Pirrone and Orazio Gambino are with Department of Computer Science, University of Palermo, building 6 - 3rd floor, Palermo (ITALY)
{ardizzon,pirrone}@unipa.it
gambino@csai.unipa.it

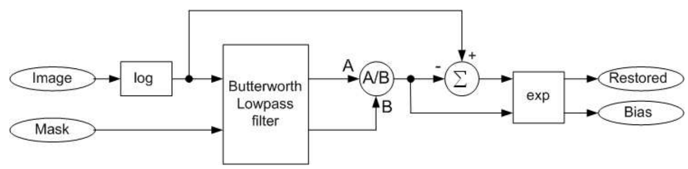

Fig. 1. The Guillemaud filter.

B. Determining Butterworth cutoff frequency

E^2D-HUM faces the main problem of the *Gf*: finding the Butterworth cutoff frequency. This problem is resolved considering the homomorphic process like an information transfer from the corrupted image to the bias one. The Shannon Entropy has been chosen as the information measure and it is computed only on the ROI of the bias image. Plotting this function with increasing values of the cutoff frequency, the bias local entropy diagram (*bled*) is obtained. Initially, it rises strongly, like a transient phase of a condenser, because most of both the image information and the artifact are located at lowest frequencies. While increasing the cutoff frequency also useful information is transferred to bias image. The Shannon Entropy is fitted using the following model:

$$y(x) = k_1 + k_2 e^{-\frac{x}{\tau}} \tag{1}$$

This operation is performed minimizing the quadratic error. In order to stop this information transfer without transferring too much information, a value of 5τ has been chosen as cutoff frequency, where the transient phase ends.

III. MORPHOLOGICAL E^2D-HUM

Dark regions inside the foreground produce streak artifact with the paradoxical result of introducing a new illumination artifact: this is another problem of *Gf*. In [1] an accurate masking is strongly recommended, instead of a coarse segmentation to define a ROI as suggested in [6]; in this way, dark regions are removed from the ROI avoiding the streak artifact after the filtering. Dark regions recognition

1-4244-0033-3/06/$20.00 ©2006 IEEE.

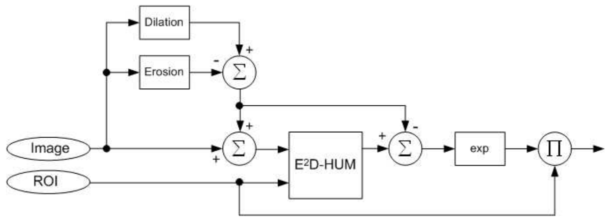

Fig. 2. $ME^2D - HUM$ scheme. $\prod$ block stands for pixel-by-pixel multiplication.

was performed by a fuzzy c-means algorithm [19] after an application of E^2D-HUM using the ROI to attenuate the bias artifact, because segmenting a bias corrupted image is useless. The basic idea consists in introducing an illumination artifact on the edges in such a way that the low pass filtering inside of *Gf* produces a low intensity variations around them. Such an artifact can be produced adding to the corrupted image the morphological gradient:

$$I' = I + (I \oplus K - I \ominus K)$$

where the symbols $\oplus$ and $\ominus$ denote the dilation and erosion morphological operations, K is the structuring element indicating the neighborhood of a pixel. For all the experiments a 3x3 squared structuring element has been chosen. Only the edges between foreground and background are preserved form this operation. The E^2D-HUM can be performed using a ROI instead of a mask and morphological gradient is subtracted from the resulting image. Finally, the background is suppressed obtaining the restored image whose dynamics is stretched to the original one. A scheme of the entire process can be found in fig.2. In order to better explain how the algorithm works, a toy problem is presented. A gray level image 255x255 has been built which is composed by a background whose intensity is 0 and a foreground made by two boxes with a gray level 128 and 120, respectively. A dark stripe, whose gray level is 0, is placed across the two regions defined above. The two closest vertical coordinates to the origin of the Fourier transform have been multiplied by 1.5 thus obtaining a synthetic bias artifact. In this way an artificial corrupting illumination has been introduced that is shaped as a white horizontal stripe as shown in fig.3.

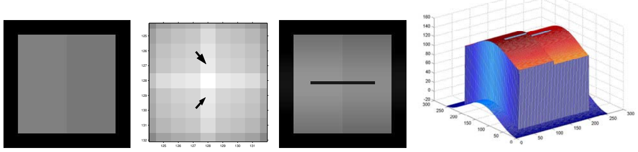

Fig. 3. The normal toy image, the spectrum with two arrows indicating the amplified low frequencies, the biased toy image with a black stripe, a 3D representation of the toy problem which shows the intensity variations.

IV. The medical evaluation and measures

The presented algorithm performs well on a large dataset of real images. The peripheral zones of the restored images

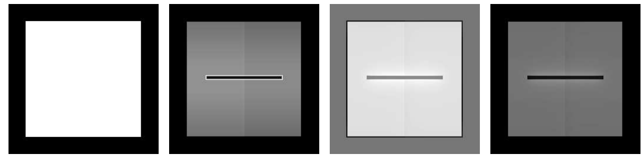

Fig. 4. From left-to-right: ROI, the original image with the added morphological gradient, after E^2D-HUM and the morphological gradient is subtracted, background suppressed and normalized.

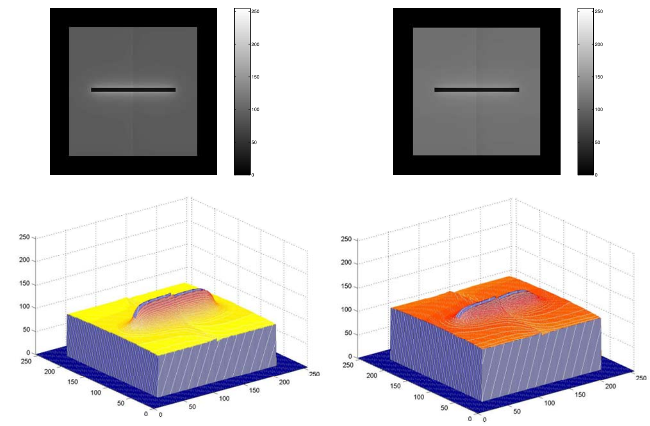

Fig. 5. UP From Left-to-Right: result using $E^2D - HUM$, the same using $ME^2D - HUM$ and the ROI. Down: the 3D representation of the results.

have been enhanced while in the original ones the central part was brighter than the rest. The filtered image doesn't exhibit false negatives or positives due to a grey levels distortion introduced by the filtering, and the boundaries between the tissues are preserved. The images restored with $ME^2D - HUM$ appear sometimes brighter than the $E^2D - HUM$ and $SPM2$ without loosing sharpness of particulars and they don't appear out of focus. After the visual inspection, an handmade segmentation of a slice has been performed to measure the coefficient of variation cv inside of the located zones and the coefficient of contrast cc between only the adjacent zones:

$$cv(zone) = \frac{\sigma(zone)}{\mu(zone)} \qquad cc(zone_1, zone_2) = \frac{\mu(zone_1)}{\mu(zone_2)}$$

where σ and μ are, respectively, standard deviation and the mean value of a segmented zone. The most used measure is cv [14][5][8] while nothing of them performs a measure on contrast, which is reduced after the application of any

a) b) c)

Fig. 6. A comparison between $E^2D - HUM$ a) and $ME^2D - HUM$ b) using the ROI c)

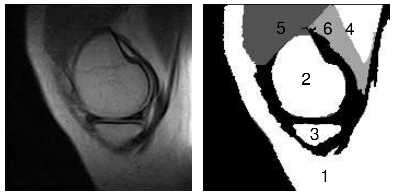

Fig. 7. Original image and labels for the measures in fig.8.

	Coefficient of variation			
	before	ME^{2}D-HUM	E^{2}D-HUM	SPM2
zone1	0.492726	0.226901	0.270068	0.240894
zone2	0.165578	0.094123	0.095581	0.097203
zone3	0.107908	0.096591	0.126117	0.101534
zone4	0.319164	0.259760	0.213492	0.205321
zone5	0.272219	0.23323	0.172129	0.170696
zone6	0.332079	0.137967	0.184323	0.127746

	Coefficient of contrast			
	before	ME^{2}D-HUM	E^{2}D-HUM	SPM2
zone1-5	2,942564	1,594823	1,789431	1,695809
zone2-5	3,153020	1,617752	1,842228	1,679237
zone5-6	2,316716	1,563483	1,787550	1,713809
zone6-4	2,259077	1,644104	1,836620	1,731609

Fig. 8. UP: E^2D-HUM, ME^2D-HUM corrected, SPM2 restored, labels. Down: Coefficient of variations and Coefficient of contrast tables.

illumination correction algorithm. As it can be seen in fig. 8, the cv table shows good performance comparing with E^2D-HUM and SPM2 algorithm[20] in some zones with a limited loss of contrast reported by cc table. The measures was performed also with E^2D-HUM because the ROI has been employed in this experimentation instead of the mask. A comparison between ME^2D-HUM and SPM2 has been also performed on a T1-weighted volume of the brain corrupted by 5% noise and 40% of rf-inhomogeneity downloaded from the simulated brain database Brainweb [21][22].

V. Experimental Setup

The method has been applied without any optical scanner acquisition which may introduce other artifacts, but the images have been decoded from DICOM file format. The device is an ESAOTE ARTOSCAN C with a magnetic field intensity of 0.18 Tesla. The dataset presented in this paper is a complete study of the knee on sagittal plane which consists of 19 T1-weighted images on 5 subjects acquired with the following parameters: Spin Echo sequence, Repetition time: 980 ms, Echo time: 26 ms, Slice thickness: 4mm, Flip Angle= 90. The FOV resolution is 170x170 pixels with 12 bit of pixel depth.

VI. Conclusions

Despite a decreasing of cc values, the contrast among the tissues is still good because it is about 160%. For example, the cc values between gray matter and white matter of an uncorrupted T1-weighted mri downloaded from Brainweb exhibits a contrast of only 130%. Moreover, the contrast of the corrupted image is altered by the artifact, so the contrast of the restored image must be lower than the original one. The cv values are comparable and sometimes better than E^2D-HUM and $SPM2$. The improvement of the algorithm isn't trivial because the fuzzy c-means requires the number of cluster as a parameter to perform the segmentation. As consequence, a trial phase must be performed to find this parameter in such a way that the cluster with lowest centroid contains dark tissues whose intensity is comparable with the background. As consequence, ME^2D-HUM is about 50% faster than E^2D-HUM. Both the algorithms have been implemented as Matlab functions using a personal computer Pentium 4 3.02 GHz with 1GB RAM.

VII. Acknowledgments

This work has been partially supported by Istituto Radiologico PIETRO CIGNOLINI - Policlinico dell'Universitá di Palermo. Particulars thanks to **Eng. Daniele Peri** for his technical support, **Dr. Gian Piero De Luca and Dr. Claudio Cusumano** for their medical support and **Dr. Prof. Giuseppe De Maria** for his availability.

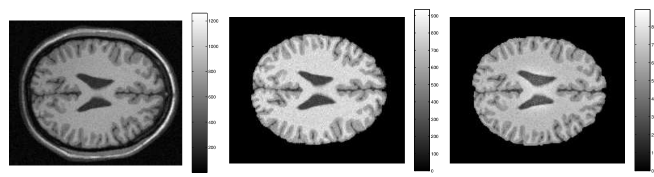

	Coefficient of contrast		
	original	ME^2 D-HUM	SPM2
wm-gm	1,3627	1,29	1,3294
gm-csf	1,8647	1,6367	1,8857
wm-csf	2,5411	2,11	2,5068

	Coefficient of variation		
	original	ME^2 D-HUM	SPM2
wm	0,0759	0,0696	0,0571
gm	0,1226	0,1074	0,1109
csf	0,5478	0,1942	0,2363

Fig. 9. Correction on Brainweb - slice98. Up From-left-to-right: original image, spm2 restored, ME^2D-HUM restored.Down: Coefficient of contrast and Coefficient of variation tables.

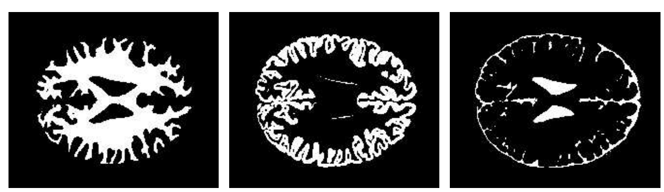

Fig. 10. The binary masks of white matter (wm), gray matter (gm) and cerebrospinal fluid (csf) provided by Brainweb. These masks have been used only for the coefficients evaluation showed in fig.9

References

[1] Ardizzone, E.; Pirrone ,R. and Gambino, O. :*Exponential Entropy Driven HUM on Knee MR Images* Proc. OF IEEE XXVII Engineering in Medicine and Biology Conference - 4/7 September 2006 SHANGHAI (CHINA)

[2] Styner, M.; Brechbuhler, C.; Szckely, G.; Gerig, G.: *Parametric estimate of intensity inhomogeneities applied to MRI Medical Imaging*. IEEE Transactions on Medical Imaging **22** (2000)153–165

[3] Shang-Hong Laia; Ming Fangb: *A dual image approach for bias field correction in magnetic resonance imaging*. Magnetic Resonance Imaging **21** (2003)121–125

[4] Mohamed N. Ahmed; Sameh M. Yamany; Nevin Mohamed: *A Modified Fuzzy C-Means Algorithm for Bias Field Estimation and Segmentation of MRI Data*. IEEE Transactions on Medical Imaging **21** (2002) 193–199

[5] Van Leemput K.;Maes F.; Vandermeulen D. and Suetens P.: *Automated Model-Based Bias Field Correction of MR Images of the Brain*. IEEE Transactions on Medical Imaging **18** (1999) 885–896

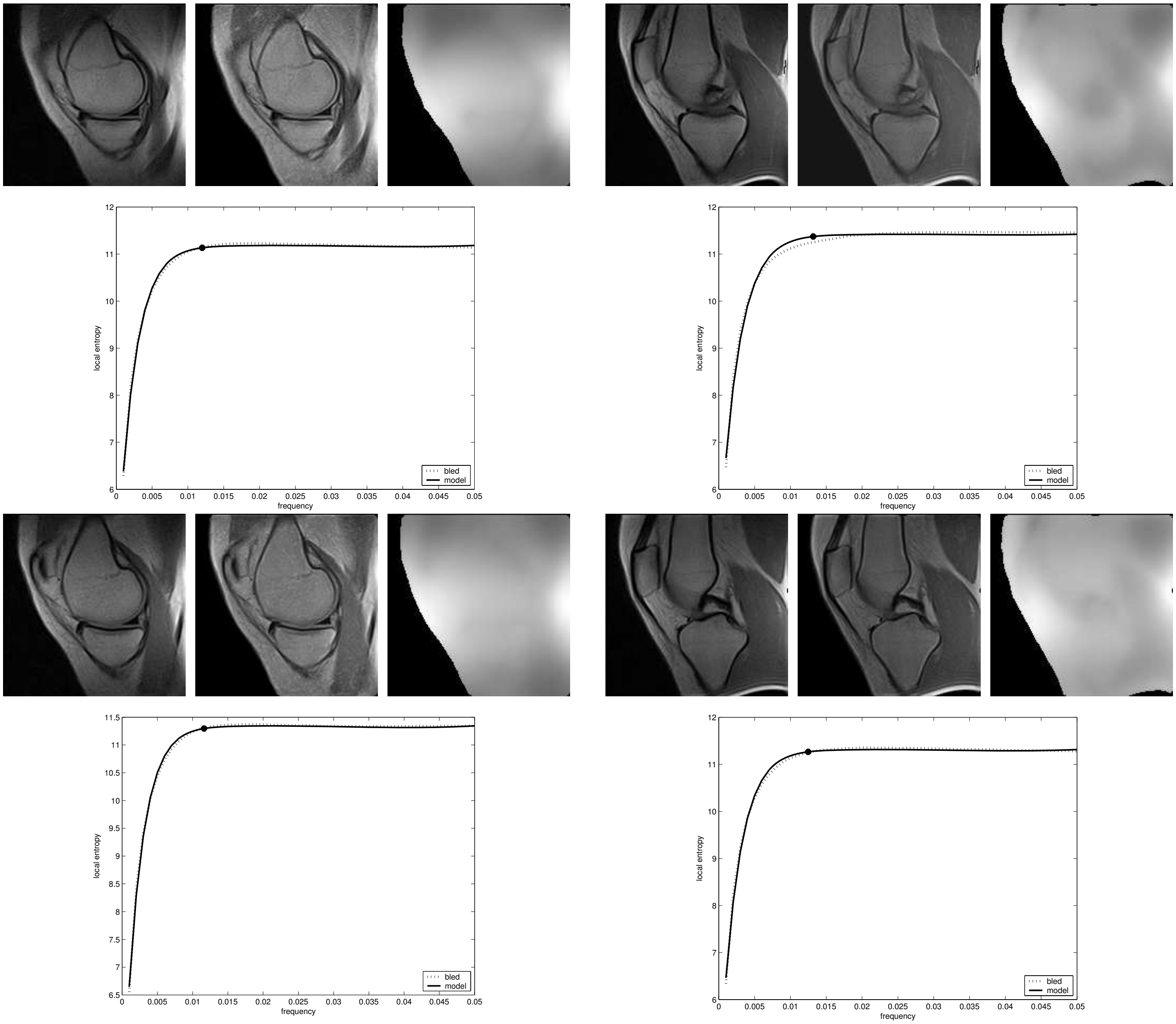

[6] Guillemaud, R.: *Uniformity Correction with Homomorphic filtering on Region of Interest*. IEEE International Conference on Image Processing **2** (1998) 872–875

[7] Guillemaud, R.; Brady, M. : *Estimating the bias field of MR images*. IEEE Transactions on Medical Imaging **16** (1997) 238–251

[8] Dawant B.M.; Zijdenbos A.P.; Margolin R.A.: *Correction of Intensity Variations in MR Images for Computer-Aided Tissue Classification*. IEEE Transactions on Medical Imaging **12** (1993) 770–781

[9] Axel L.; Costantini J.; Listerud J.: *Intensity Correction in Surface Coil MR Imaging*. American Journal on Roentgenology **148** (1987) 418–420

[10] Lei Jiang,Wenhui Yang:*A Modified Fuzzy C-Means Algorithm for Segmentation of Magnetic Resonance Images*. Proc. VIIth Digital Image Computing: Techniques and Applications.Sun C., Talbot H., Ourselin S. and Adriaansen T. Editions. (2003) 225–231

[11] Tincher M.; Meyer C.R.; Gupta R.; Williams D.M.: *Polynomial Modelling and Reduction of RF Body Coil Spatial Inhomogeneity in MRI*. IEEE Transactions on Medical Imaging **12** (1993) 361–365

[12] Brinkmann B. H. , Manduca A. and Robb R. A.: *Optimized Homomorphic Unsharp Masking for MR Grayscale Inhomogeneity Correction*. IEEE Transactions on Medical Imaging. **17** (1998) 161–171

[13] Wells W.M.; Grimson W.E.L.; Kikins R.; Jolez F.A.: *Adaptive Segmentation of MRI Data*. IEEE Transactions on Medical Imaging. **15** 429–442 (1996)

[14] Likar B.; Viergever M.A.; Pernus F.: *Retrospective Correction of MR Intensity Inhomogeneity by Information Minimization*. IEEE Transactions on Medical Imaging **20** (2001) 1398–1410

[15] Vovk U., Pernus F. and Likar B.: *Multi-feature Intensity Inhomogeneity Correction in MR Images.* Proc. of MICCAI 2004 "Lecture Notes in Computer Science" vol. 3217 283-290

[16] Pham D.L.; Prince J.L.: *Adaptive Fuzzy Segmentation of Magnetic Resonance Images*. IEEE Transactions on Medical Imaging. 18(9), (1999) 737-752

[17] Hernández J.A., Mora M.L., Schiavi E., and Toharia P. :*RF Inhomogeneity Correction Algorithm in Magnetic Resonance Imaging* ISBMDA 2004, LNCS 3337, pp. 18, 2004

[18] Arnold JB; Liow J-S; Schaper KS; Stern JJ; Sled JG; Shattuck DW; Worth AJ; Cohen MS; Leahy RM; Mazziotta JC; Rottenberg DA. *Quantitative and Qualitive Evaluation of Six Algorithms for Correcting Intensity Non-Uniformity Effects.* Neuroimage (2001) 13(5) 931–943.

[19] Bezdek J.C. :*Pattern Recognition with Fuzzy Objective Function*. Plenum Press 1981.

[20] www.fil.ion.ucl.ac.uk/spm/software/spm2/

[21] http://www.bic.mni.mcgill.ca/brainweb/

[22] D.L. Collins, A.P. Zijdenbos, V. Kollokian, J.G. Sled, N.J. Kabani, C.J. Holmes, A.C. Evans : *Design and Construction of a Realistic Digital Brain Phantom* IEEE Transactions on Medical Imaging, vol.17, No.3, p.463–468, June 1998